Mon. Not. R. Astron. Soc. **304,** 319–326 (1999)

Segregated optical–near-infrared colour distributions of Medium Deep Survey galaxies

I. Ferreras,[1,2] L. Cayón,[2] E. Martínez-González[2] and N. Benítez[3]

[1]*Departamento de Física Moderna, Universidad de Cantabria, 39005 Santander, Spain*
[2]*Instituto de Física de Cantabria, Fac. Ciencias, Av. los Castros s/n, 39005 Santander, Spain*
[3]*Astronomy Department, University of California, Berkeley, CA 94720, USA*

Accepted 1998 November 17. Received 1998 September 15; in original form 1998 May 29

ABSTRACT

We present a K survey of 29 fields covering approximately 90 arcmin^2 from the Medium Deep Survey (MDS) catalogue down to a completeness magnitude of $K = 18.0$ (limiting magnitude $K = 19.0$). The morphology obtained by the MDS team using high-resolution images from *HST*/WFPC2 along with our near-infrared (NIR) observations allows colour–magnitude and colour–colour analysis that agrees in general with spectral evolution models, especially if a reasonable range of metallicities for the simple stellar populations used ($0.2 < Z/Z_{\odot} < 2.5$) is considered. However, a significant population of *spheroids* was found, which appears *bluer than expected*, confirming previous observations. This blueness might possibly signal the existence of non-negligible star formation in ellipticals and bulges at medium redshift. A number counts calculation for different morphological types shows that discs become the dominant population at faint magnitudes. The median redshift of the sample is $z \sim 0.2$, from a photometric redshift estimation using $V - K$ and $I - K$. A search for Extremely Red Objects (EROs) in the survey field was also performed, with no detection of objects having $I - K > 4.5$, setting an upper limit to the number density of EROs $\mathrm{d}n_{\mathrm{EROs}}/\mathrm{d}\Omega < 0.011$ arcmin^{-2} ($K \leq 18.0$).

Key words: surveys – galaxies: evolution – cosmology: observations – infrared: galaxies.

1 INTRODUCTION

With the advent of the *Hubble Space Telescope* (*HST*), observational cosmology has been capable of extending the study of galaxy formation and evolution to epochs corresponding to less than one third of the age of the Universe. The extremely narrow point spread function (PSF) produced by *HST*/WFPC2 images (around 0.1 arcsec) allows morphological classifications of galaxies at medium to high redshifts. The Medium Deep Survey (MDS) key project (Griffiths et al. 1994) has been classifying field galaxies from hundreds of WFPC2 images, providing photometry in two bands (F606W and F814W, which roughly correspond to standard V and I, respectively) as well as morphology down to $I \sim 22.0$. These data allow the study of number counts selected by type in the I and V bands (Glazebrook et al. 1994; Driver, Windhorst & Griffiths 1995; Abraham et al. 1996). The results indicate that counts in elliptical and spiral galaxies match closely the predictions of non-evolving models, whereas the population of irregular/peculiar galaxies presents an excess over no-evolution estimations. The median redshift for spectroscopically confirmed galaxies is $z = 0.5$.

Inside knowledge of formation and evolution processes conforming the observed field galaxy population mixture requires additional data. Spectroscopic studies will provide intrinsic luminosities as well as information about absorption and emission lines. Also, optical–infrared colours are sensitive to the stellar population content. Optical emission comes mostly from young OB stars while the old stellar population dominates the infrared luminosity. In a recent paper, Glazebrook et al. (1998) study the characteristics of the faint MDS population through optical spectroscopy and near-infrared photometry. An excess of blue ellipticals is found in $I - K$ distributions compared with pure luminosity evolution models. The main purpose of this work is to study the characteristics of normal galaxies in MDS fields through optical–infrared colours.

This paper is organized as follows. A detailed account of the observations and data reduction processes is presented in Section 2. We present the number counts in the K' band, compare them with previous observations and discuss the morphologies contributing at different magnitudes in Section 3. Sections 4 and 5 are dedicated to optical–infrared colour relations, the latter focusing on the blue spheroid population found. A search for Extremely Red Objects (EROs) is presented next. Finally, a discussion of our results is presented in Section 7.

2 OBSERVATIONS AND DATA REDUCTION

The targets for our K'-band survey were chosen from the Medium Deep Survey catalogue, which can be accessed at the *HST*/MDS Archive (http://archive.stsci.edu/mds/mds.cgi). Our search was

Table 1. MDS/MAGIC survey fields.

Field	RA (J2000.0)	Dec. (J2000.0)
uqk00	07 42 44.0	+65 06 08.0
usp00	08 54 16.0	+20 03 41.0
uzp00	11 50 29.0	+28 48 27.0
uzk03	12 10 34.0	+39 28 53.0
uzx01	12 30 54.0	+12 19 05.0
uz 00	13 00 23.0	+28 20 13.0
u26x1	14 15 20.0	+52 03 01.0
u26x2	14 15 14.0	+52 01 50.0
u26x3	14 15 07.0	+52 00 40.0
u26x9	14 17 23.0	+52 25 13.0
u26xa	14 17 17.0	+52 24 03.0
u26xb	14 17 10.0	+52 22 53.0
u26xc	14 17 04.0	+52 21 43.0
u26xd	14 16 57.0	+52 20 33.0
u26xe	14 16 51.0	+52 19 23.0
u26xf	14 16 44.0	+52 18 13.0
u26xg	14 16 38.0	+52 17 03.0
u26xh	14 16 31.0	+52 15 53.0
u26xi	14 16 25.0	+52 14 43.0
u26xj	14 16 18.0	+52 13 32.0
u26xk	14 16 12.0	+52 12 22.0
u26xl	14 16 05.0	+52 11 12.0
u26xm	14 15 59.0	+52 10 02.0
u26xn	14 15 52.0	+52 08 52.0
u26xo	14 15 46.0	+52 07 42.0
u26xp	14 15 39.0	+52 06 31.0
u26xq	14 15 33.0	+52 05 21.0
u26xr	14 15 27.0	+52 04 11.0
ux400	15 19 41.0	+23 52 05.0

based on optimal positioning in the sky for our observing time and place, taking extra care not to bias the catalogue towards regions nearby quasars, active galaxies or other peculiar objects. We found a set of images taken under *HST* programme GTO5090 (with E. Groth as Principal Investigator) out of which 22 fields were selected. K'-band images of the MDS fields were obtained at the 2.2-m MPIA telescope on Calar Alto, Spain, during the nights of 1997 February 18, 20 and May 21, with MAGIC, a NIR camera that uses a NICMOS3 256^2 Rockwell HgCdTe array, with a pixel scale of 0.64 arcsec. We used the K' filter instead of standard K to reduce the sky background, thereby reaching a fainter limiting magnitude. The difference between K and K' stays below 0.01 mag if we consider the translation formula of Wainscoat & Cowie (1992) and a colour $H-K$ of a typical galaxy, given by a synthetic model (Bruzual & Charlot, in preparation). Hence, we will denote our K' magnitudes by K hereafter.

5-s individual exposures were taken, adding up groups of 12 of them into a single 1-min file. Between frames we nodded the telescope in steps of 10 arcsec, following a path that closed in 9 steps. Each field has three such sets totalling 27 min of integration time. Several UKIRT faint photometric standard stars were also imaged throughout each night. The fields were flat-fielded using the median of the set of images for each field excluding that of the frame being processed. The complete sample comprises 29 fields (Table 1) which cover a 116.8 arcmin^2 region in the K band, with an 89.4 arcmin^2 overlap with the *HST*/WFPC2 images. A translation from the *HST*/WFPC2 filters to standard V and I photometry is done using the transformation formulae from Holtzman et al. (1995) and approximating $V-I$ to F606W−F814W. The additional correction terms are less than 0.01 mag.

Table 2. Survey properties.

Band	Comp. mag.	Objects	Spheroid (%)	Disk (%)
F606W (V)	$V<21.8$	276	9.8	62.7
F814W (I)	$I<21.0$	377	15.1	53.8
$I+K$	$K<18.0$	170	18.0	40.0
$V+I+K$	$K<18.0$	109	14.0	45.0

The object detection process was done using SExtractor (Bertin & Arnouts 1996) using a $2.5\sigma/\sqrt{N}$ detection threshold, where N is the number of connected pixels within one seeing disc. Hence, the global threshold is 2.5σ. Even though this value might be rather low for individual band detection, we are only considering those objects that appear in *both* the K and MDS I or V images. We compared the aperture and isophote-fitting photometry from SExtractor and IRAF's QPHOT task using 4-, 5- and 6-arcsecond discs and found the maximum uncertainty to lie around 0.2 mag down to a limiting magnitude of $K=19$. Eventually, we decided to use 6-arcsec aperture photometry, which guarantees that all of the flux from each object is measured. Moreover, this is the same aperture used by Glazebrook et al. (1998), which allows a better comparison.

In order to match the WFPC2 and MAGIC images, we retrieved individual *HST* frames for each field from the STScI archive (with exposure times around 1 000 s) and compared them with our NIR images. We took several objects in each field to find the pixel-to-coordinate mapping. Many of the images used in the survey overlap, and so we checked for objects appearing twice. Table 2 shows the number of objects detected as well as the ratio of spheroids and discs in the sample (bulge-to-disc ratio >0.75 and <0.25 respectively). As expected, the bias in imposing detection in all bands V,I and K implies a higher proportion of discs, compared with only imposing I and K detection.

The completeness magnitude was estimated in two different ways. A quick method involves searching for the peak in the histogram of objects appearing both in K and I bands to make sure we are rejecting spurious detections. This method is only possible as long as we are working with images that are much deeper in I than in K, so that no severe bias is included by enforcing I-band detection. Also, the peak of the histogram will only show the completeness level as long as the luminosity function is monotonically increasing in the detection range (which is the case for us; see, for instance, Fig. 1). The second method consists of simulating a random field of point-like galaxies with the luminosity function obtained from the literature (cf. Fig. 1) and with the same sky noise and pixel size. We could have considered a sample of spheroids and discs in the simulated sample, as the threshold of detection deals with surface brightness; however, most of the galaxies from the MDS catalogue had half-light radii well below 1.5 arcsec (see, for instance, Table 3), which was our resolution taking into account seeing conditions and pixel size. Both methods yielded a completeness magnitude of $K=18.0$.

3 NIR NUMBER COUNTS AND MORPHOLOGY

We construct the number counts in the NIR with the objects detected by SExtractor in the MAGIC images which have

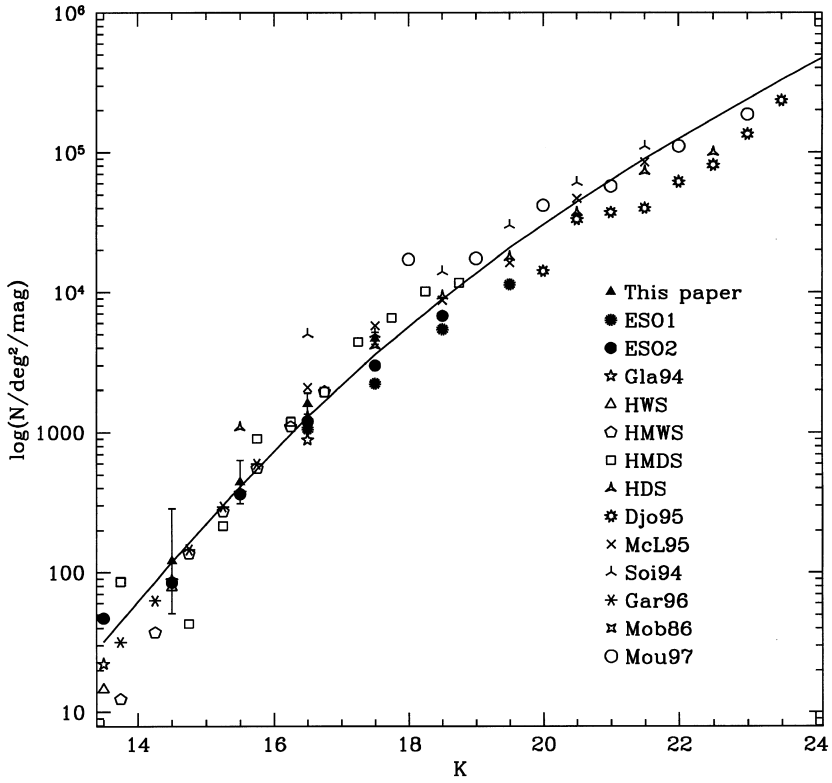

Figure 1. *K*-band number counts compared with those of previous surveys. The solid line corresponds to a no-evolution model. The solid triangles represents our results for objects detected *both* in I (< 22) and K (< 18). Poisson error bars are shown.

Table 3. Spheroids from the MDS/MAGIC survey.

ID	F814W	F606W−F814W	F814W−K	r_{HL}(arcsec)	B/T	Field
E1	19.83	0.83	2.97	0.37	1.00	uqk00
E2	19.75	1.80	3.70	0.52	0.82	uzk03
E3	20.47	1.50	3.10	0.37	1.00	uzk03
E4	19.42	1.46	3.03	0.49	0.76	u26x1
E5	20.19	1.63	2.69	0.29	1.00	u26x1
E6	19.75	1.02	2.23	0.90	1.00	u26x1
E7	20.24	1.59	3.61	0.32	0.79	u26xq
E8	18.01	1.29	3.13	0.88	0.87	u26xj
E9	20.27	1.13	3.14	0.29	1.00	u26xj
E10	19.33	0.94	2.92	0.32	1.00	u26xi
E11	20.61	1.18	2.91	0.19	0.83	u26xi
E12	20.08	1.95	3.49	0.53	1.00	u26xg
E13	17.20	1.14	2.66	0.13	1.00	u26xd
E14	20.38	1.53	3.39	0.34	0.85	u26xd
E15	20.69	1.14	1.95	0.58	1.00	u26xc

counterparts in MDS I-band frames. Even though this might appear as a severe bias on the sample, it is not, as can be seen in Fig. 1, where our $I+K$ sample is shown along with data from the literature. A strong bias would appear as a paucity of objects and thus a disagreement with previous K-band surveys. The only population that might drop out in this process would consist of blue irregular galaxies, which contribute negligibly to the luminosity function in our magnitude range ($K \leq 18$).

The counts follow a $\mathrm{d}\log N/\mathrm{d}m$ relation with a slope of ~0.4 in the range $16 \leq K \leq 18$. Differential number counts versus K magnitude of our sample are presented in Fig. 1 (solid triangles), along with Poissonian error bars. Just for comparison, a no-evolution model (solid line) based on the luminosity function given by Efstathiou, Ellis & Peterson (1988) is also presented. We assume a cosmology with $\Omega_0 = 0$ and $H_0 = 50\,\mathrm{km\,s^{-1}\,Mpc^{-1}}$ and a galaxy mixture [including star formation rates (SFRs) and initial mass function (IMFs)] as prescribed by Pozzetti, Bruzual & Zamorani

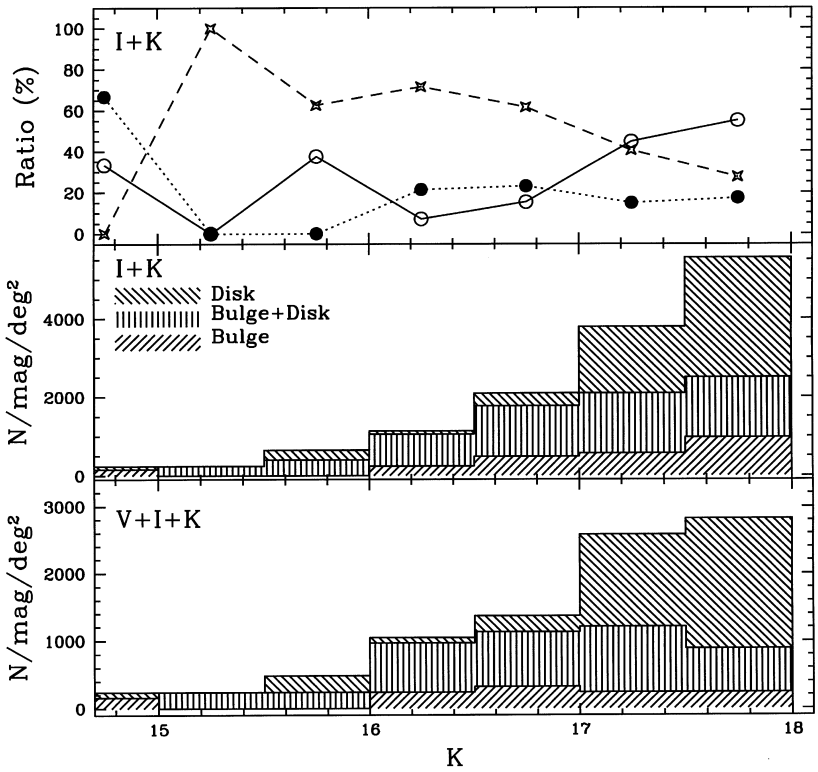

Figure 2. Evolution of morphology types as a function of K-band apparent magnitude (i.e. approximately as a function of redshift). The top panel gives the ratio of each type to the total. Solid circles: bulges; stars: bulge+disc; hollow circles: discs.

(1996). The k-corrections and colours are calculated for different types of galaxies using the spectral synthesis code from Bruzual & Charlot (in preparation). The model has been normalized to the observations from the literature at $18 < K < 18.5$ (the present sample not included). The no-evolution model is compatible with the observations down to our completeness magnitude. Moreover, the NIR number counts down to $K \sim 20$ cannot discriminate between no-evolution and passive luminosity evolution models (Pozzetti et al. 1996). On the other hand, the slope of the K-band number counts seems to flatten for the faintest magnitudes (Djorgovski et al. 1995; Moustakas et al. 1997).

Unlike many previous K-band surveys, now we have access to the morphology of the objects from the I- and V-band images classified by the MDS group. Figs 2 and 3 serve as a test of the contribution from each morphology to the counts in different bands. We plotted in Fig. 3 the fraction of the total number of galaxies detected in I and K (top) and in V, I and K (bottom) versus the bulge to total luminosity ratio measured in I. As in a typical field sample, the proportion of disc galaxies is higher than that of bulges. The percentage of the latter ($B/T > 0.75$) is smaller in the sample selected in V,I and K than in the one selected in I and K alone. This result follows the ratios observed in the MDS objects in the two filters I and V (see Table 2). From Fig. 2 (top), one can see that the ratio of bulges in field galaxies decreases as we go to fainter magnitudes, down to $\sim$1/10 at $K = 18.0$, whereas the disc population comprises roughly 60 per cent of the sample at the faint end. The contribution of the different populations to the differential number counts at different K magnitudes is presented in Fig. 2 (middle and bottom panels). One can see in both panels the trend indicated above: faint magnitude counts are clearly dominated by discs.

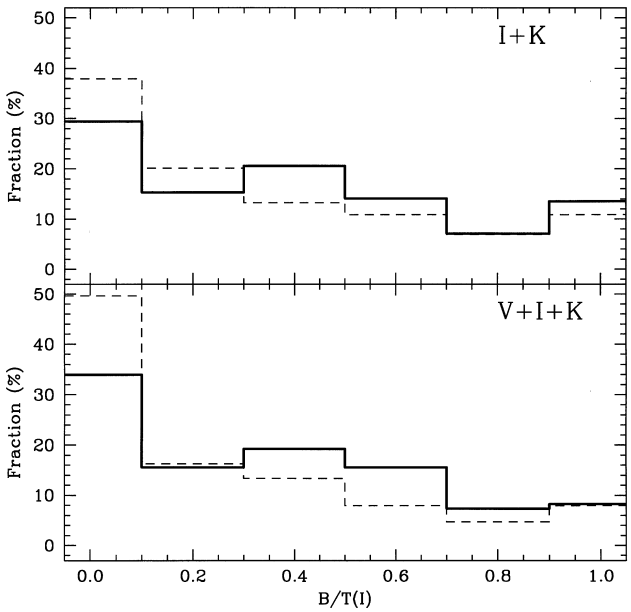

Figure 3. Bulge-to-total fractions in $I + K$ and $V + I + K$ selected samples (solid lines). The dashed lines represent the histogram without the constraint of K-band detection.

4 COLOUR–MAGNITUDE RELATIONS

Figs 4(a) and (b) show the colour–magnitude relation for our sample in $V - K$ and $I - K$. Having the morphology of each object, we can go further and predict the colours that galaxies

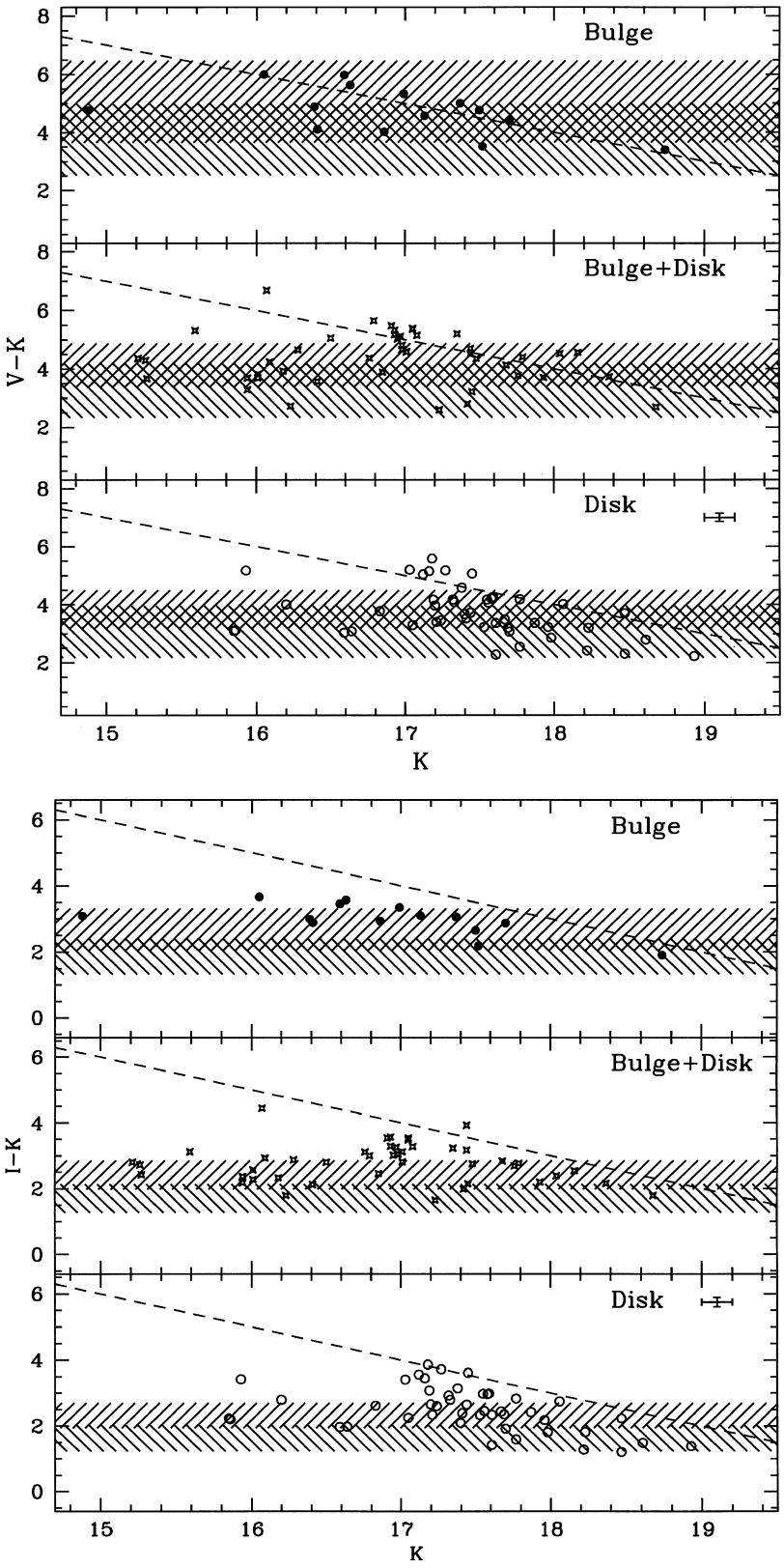

Figure 4. (a) $V - K$ and (b) $I - K$ colour–magnitude relations. The shaded area spans the colour region predicted by a model from Bruzual & Charlot (in preparation), between redshifts $0 < z < 1$ for two metallicities: $2.5\,Z_{\odot}$ (redder region) and $Z_{\odot}/5$ (bluer region). The dashed line shows the completeness limit in (a) V or (b) I. A conservative error bar (i.e. the typical error for objects at the completeness magnitude) appears in the bottom panel. Details of the models used appear in the paper.

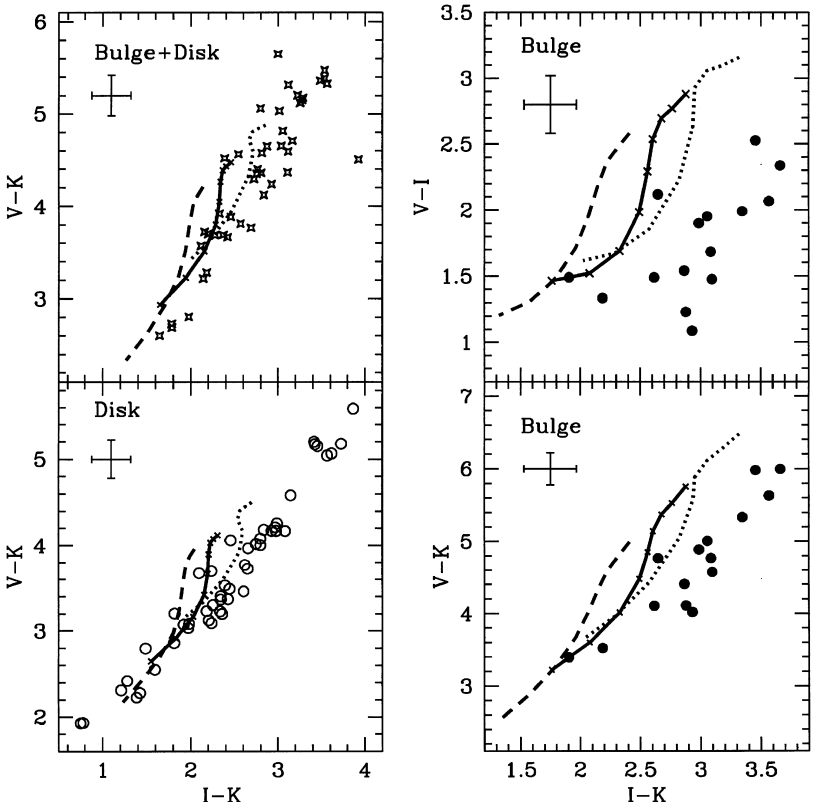

Figure 5. Colour–colour plots. The lines correspond to model predictions from Bruzual & Charlot (in preparation) for three different metallicities: $2.5\,Z_\odot$ (solid), $Z_\odot$ (dotted), and $Z_\odot/5$ (dashed). A formation redshift $z_F = 5$ is assumed and each type only differs in the SFR time-scale: $\tau = 1, 5, \infty$ Gyr for B, B+D and D, respectively. The typical error bar at the completeness level is also shown for each diagram.

with a given morphology should have. The shaded regions in these figures show the range of colours expected for galaxies with redshift $0 < z < 1$, according to the models of Bruzual & Charlot (in preparation) for two metallicities: one higher than solar ($2.5\,Z_\odot$) and another lower than solar ($Z_\odot/5$). All of them have a Scalo IMF defined for $0.1\,M_\odot < M < 100\,M_\odot$ and an exponential SFR with a characteristic time τ. The morphology determines the value of τ: 1 Gyr for bulges, 5 Gyr for bulge + disc and ∞ (i.e. constant SFR) for discs. The formation redshift for all three models is $z_F = 5$. Given the degeneracy that exists between age and metallicity (e.g. Worthey 1994), we can account for a range of colours either by changing the formation redshift or by using different metallicities. In the figures we used the latter approach: we can see that a lower metallicity shifts the colour blueward in the same way a lower formation redshift would.

Unfortunately, we do not know the redshifts of these galaxies and so we cannot compare the trajectory predicted by the models with the colours of MDS galaxies. One is tempted, though, to use a $K - z$ relation from deep surveys (Cowie et al. 1996); however the spread in this relation is too large to produce a meaningful result. A colour–colour plot avoids the estimation of redshift, and is shown in Fig. 5. The dotted, solid and dashed lines correspond to three different metallicities, namely $Z/Z_\odot = 2.5$, 1.0 and 0.2, respectively. The solar metallicity curve also gives the redshift as crosses, from $z = 0$ (blue–blue i.e. lower left-hand corner) up to $z = 1$ in steps of $\Delta z = 0.1$. There is good agreement with the colour–colour trend for all three morphologies, although a range of metallicities (or of formation redshifts) is needed to account for quite a few of the galaxies. It is worth mentioning this issue as either age or

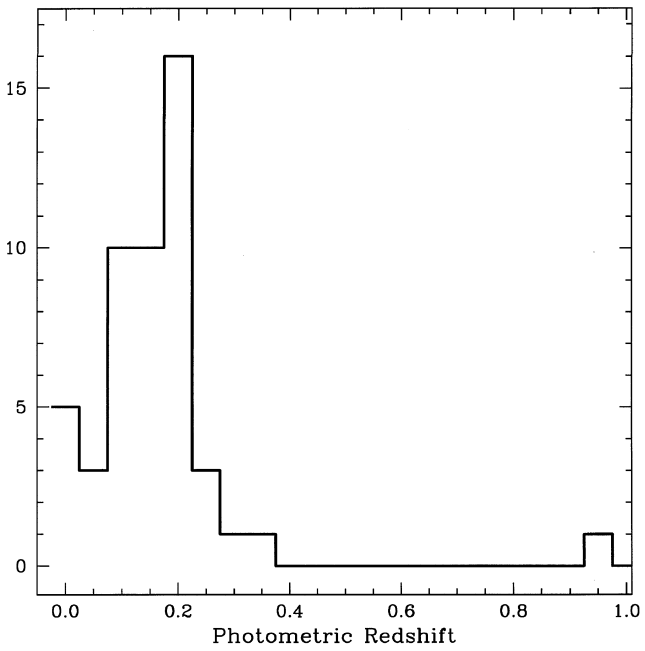

Figure 6. Histogram of the photometric redshift estimated for objects detected in V, I and K using the predictions for $V - K$ and $I - K$ from the models of Bruzual & Charlot (in preparation). The median redshift is $z_{PHOT} \sim 0.2$.

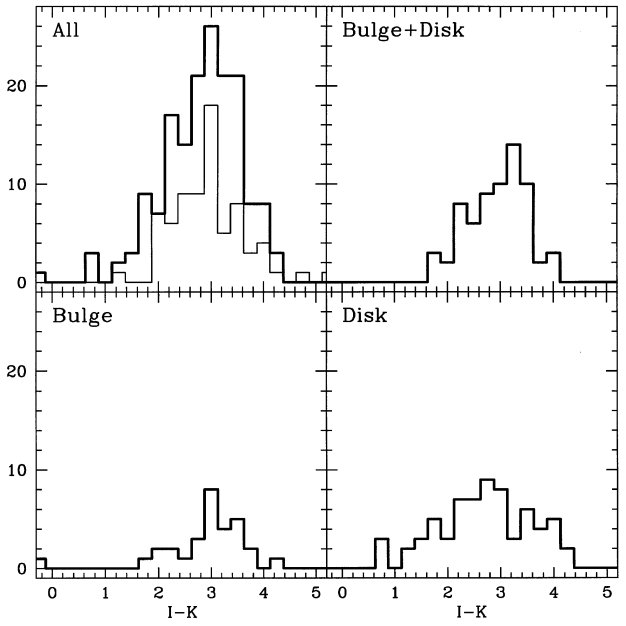

Figure 7. $I-K$ colour histogram as a function of morphology. The thin line shows the histogram from Glazebrook et al. (1998), which is scaled down to fit the box limits.

metallicity can account for this range of colours. The few discs with red $V-K$ and $I-K$ colours in Fig. 5, which fall away from the model predictions, should be considered with care as they fall close to the detection limit in V and I and so the photometric error in these bands could be large. The result for spheroids is treated in the next section.

Finally, we left as an interesting exercise computing the values estimated for the redshift using a purely photometric approach. This method compares the broad-band colours with templates associated with the morphology of the galaxy, shifting the redshift until the predicted colours are compatible with the observations. The more bands used, the better estimation one should have. Photometric redshift measurements can be thought of as a 'poor man's spectroscopy'. Previous work on the subject has achieved remarkable accuracy: Brunner et al. (1997) performed a multiband analysis which resulted in a dispersion $\Delta z \sim 0.02$ up to $z = 0.4$. A deeper estimation of the uncertainties can be found in Hogg et al. (1998).

In our case, we only have two colours ($V-K$ and $I-K$), which drove us to use a simple method to estimate the redshift, namely minimizing the squared difference between predicted and observed colours, using for each morphological type the models described above with three different metallicities. We imposed as a valid estimation that which corresponded to a colour difference less than ± 0.5 mag, which reduced the sample to roughly 45 per cent. A histogram of the objects can be seen in Fig. 6, which has a median around $z \sim 0.2$. Even though the value for the complete MDS sample is 0.5, our lower redshift is reasonable as the NIR survey described in the present work is only complete down to $K = 18$.

5 BLUE SPHEROIDS IN THE FIELD

The right-hand panels of Fig. 5 plot the spheroids in two different colour–colour diagrams. In both cases the observations fall blueward of the passive evolution estimations from spectral evolution models. This is proof of the existence of ongoing star formation. Also, the mismatch is larger in $V-K$ than in $I-K$, possibly a sign that there is more flux into V – i.e. rest-frame U and B – accounted for by young stars. Although the environment is totally different, this blueness is in agreement with the colours of some cluster ellipticals (e.g. Couch & Sharples 1987) for which a recent episode of star formation must be considered in order to explain it (Charlot & Silk 1994). Confirmation of the existence of blue ellipticals in MDS fields appears in spectroscopic observations using the Keck telescope (Forbes et al. 1996; Koo et al. 1996). We inspected visually all the spheroids in our sample and found only one possible misclassified object, which appears as a late-type galaxy. The list of all 15 spheroids with their properties appears in Table 3. These blue early-type galaxies should be studied further as they might throw light on the galaxy formation process both in the field and in clusters.

6 SEARCHING FOR EROs

A search for Extremely Red Objects (EROs) was also undertaken on this sample. First of all we checked that none of the objects found in *both* the K-band images and the *HST*/MDS catalogue from the I-band frames had a colour characteristic of such sources ($I-K > 4.5$). Next, we considered those objects from our K-band images alone that did not appear in the MDS catalogue and visually inspected both the NIR and the *HST*/MDS images (the latter retrieved through the archive of the STScI). About half of the candidates detected in K fell in a region which did not overlap with the *HST* I or V images. The other half had counterparts which were either very bright stars or galaxies that failed to adjust to the predetermined luminosity profiles. In either case, these objects were brighter than $I \sim 21$ and so they had $I-K < 3$, i.e. bluer than the standard criterion for an ERO ($I-K > 4.5$). Hence, all the objects detected in our K-band images – at a completeness level of $K = 18$ – had counterparts in I and had colours $I-K < 4.5$. The sample extends over 89.4 arcmin^2 ,which sets an upper limit for the number density of EROs at $\mathrm{d}n_{\mathrm{EROs}}/\mathrm{d}\Omega < 0.011$ arcmin^{-2} (for $K \leq 18$).

7 DISCUSSION

In this paper we have performed NIR photometry in 29 fields from the Medium Deep Survey catalogue. The number counts obtained (Fig. 1) for objects detected in *both* I- and K-band frames agree well with previous K-band surveys. This agreement is possible since the I-band images are deeper. The morphology obtained with high-resolution images from *HST*/WFPC2 allows a segregated study of colour–magnitude and colour–colour relations for three different types according to the bulge-to-disc ratios. As expected, spheroids appear redder in $V-K$ and $I-K$ than discs and there is a fairly good agreement with spectral evolution models (Bruzual & Charlot, in preparation) using a formation redshift $z_{\mathrm{F}} = 5$ and taking into account a sensible range in metallicities ($0.2 < Z/Z_{\odot} < 2.5$), which is equivalent to assuming a range in formation redshift, keeping a fixed metallicity. A simple photometric redshift estimation was performed, giving a median redshift $z \sim 0.2$, which is reasonable given the completeness level of the K-band images. A further analysis along these lines would require fluxes in additional bands.

In agreement with previous observations, we found that spheroids appear bluer than the model prediction for passive evolution, clearly showing the existence of ongoing star formation, similarly to the blueness detected in some cluster ellipticals. Further study of this epoch of possibly strong star formation in the life of early-type

galaxies will be of great importance in the understanding of galaxy formation.

In order to compare our results with those of previous NIR surveys in MDS fields (Glazebrook et al. 1998), Fig. 7 shows the histogram of objects detected in I and K along with the data from Glazebrook et al., cutting their list at our completeness level. There is very good agreement between both surveys, normalizing to the same area. A rank correlation test applied to both histograms yielded a 100 per cent confidence level. It is also interesting to notice that the extra objects in Glazebrook's sample appear blueward of the peak as they go deeper in K, signalling the existence of galaxies with a stronger star formation rate, as expected for higher redshift galaxies.

Finally, a search for EROs was undertaken on the overlapping 89.4 arcmin^2 region that had photometry in V, I, and K. The whole sample down to $K = 18$ had counterparts in the F814W frames, all with unconspicuous $I - K < 4.5$ colours. Hence, no ERO was found, yielding an upper limit for the number density of roughly $\mathrm{d}n_{\mathrm{EROs}}/\mathrm{d}\Omega < 0.011$ arcmin^{-2} ($K < 18.0$), which agrees with previous estimates (Hu & Ridgway 1994).

ACKNOWLEDGMENTS

The authors are grateful to the anonymous referee for helpful suggestions, S. F. Sánchez for pointing out valuable hints, J. M. Diego for the help provided during the last run of observations, and P. Saracco for providing us with the number count data presented in Fig. 1. We also acknowledge helpful discussions with F. Hammer and J. Silk. The 2.2-m telescope is operated by the Max Planck Institut für Astronomie at the Centro Astronómico Hispano Alemán in Calar Alto (Almería, Spain). The Medium Deep Survey catalogue is based on observations with the NASA/ESA *Hubble Space Telescope*, obtained at the Space Telescope Science Institute, which is operated by the Association of Universities for Research in Astronomy, Inc., under NASA contract NAS5-26555. The Medium Deep Survey is funded by STScI grant GO2684. IF acknowledges a a PhD scholarship from the 'Gobierno de Cantabria'. NB is supported by a Basque Government fellowship. The authors acknowledge financial support from the Spanish DGES under contract PB95-0041.

REFERENCES

Abraham R. G., van den Bergh S., Glazebrook K., Ellis R. S., Santiago B. X., Surma P., Griffiths R. E., 1996, ApJS, 107, 1
Bertin E., Arnouts S., 1996, A&AS, 117, 393
Brunner R. J., Connolly A. J., Szalay A. S., Bershady M. A., 1997, ApJ, 482, 21
Charlot S., Silk J., 1994, ApJ, 432, 453
Couch W. J., Sharples R. M., 1987, MNRAS, 229, 423
Cowie L., Songaila A., Hu E., Cohen J. G., 1996, AJ, 112, 839
Djorgovski S. et al., 1995, ApJ, 438, L13 (Djo95)
Driver S. P., Windhorst R. A., Griffiths R., 1995, ApJ, 453, 48
Efstathiou G., Ellis R. S., Peterson B. A., 1988, MNRAS, 232, 431
Forbes D. A., Phillips A. C., Koo D. C., Illingworth G. D., 1996, ApJ, 462, 89
Gardner J. P., Cowie L. L., Wainscoat R. J., 1993, ApJ, 415, L9 (HWS, HMWS, HMDS, HDS)
Gardner J. P., Sharples R. M., Carrasco B. E., Frenck C. S., 1996, MNRAS, 282, L1 (Gar96)
Glazebrook K., Peacock J., Collins C., Miller L., 1994, MNRAS, 266, 65 (Gla94)
Glazebrook K., Ellis R. S., Santiago B. X., Griffiths R. E., 1995, MNRAS, 275, L19
Glazebrook K., Abraham R., Santiago B., Ellis R., Griffiths R., 1998, MNRAS, 297, 885
Griffiths R. et al., 1994, ApJ, 437, 67
Hogg D. W. et al., 1998, AJ, 115, 1418
Holtzman J. A., Burrows C. J., Casertano S., Hester J. J., Trauger J. T., Watson A. M., Worthey G., 1995, PASP, 107, 1065
Hu E. M., Ridgway S. E., 1994, AJ, 107, 1303
Koo D. C. et al., 1996, ApJ, 469, 535
McLeod B. A., Bernstein G. M., Reike M. J., Tollerstrup E. V., Fazio G. G., 1995, ApJS, 96, 117 (McL95)
Mobasher B., Ellis R., Sharples R., 1986, MNRAS, 223, 11 (Mob86)
Moustakas L. A., Davis M., Graham J. R., Silk J., Peterson B. A., Yoshii Y., 1997, ApJ, 475, 445 (Mou97)
Pozzetti L., Bruzual G. A., Zamorani G., 1996, MNRAS, 281, 953
Saracco P., Iovino A., Garilli B., Maccagni D., Chincarini G., 1997, AJ, 114, 887 (ESO1, ESO2)
Soifer B. T. et al., 1994, ApJ, 420, L1 (Soi94)
Wainscoat R. J., Cowie L. L., 1992, AJ, 103, 332
Worthey G., 1994, ApJS, 95, 107

This paper has been typeset from a TEX/LATEX file prepared by the author.